

Effect of fire-induced water repellency on soil hydraulic properties and water flow

Lana FILIPOVIĆ¹ (✉)

Mirel MEŠIĆ¹

Thomas WENINGER²

Andreas SCHWEN²

Alen NOVOSEL¹

Matej MARETIĆ¹

Vilim FILIPOVIĆ¹

Summary

Water infiltration into the root zone, its retention in soil and drainage from the soil profile, are highly sensitive to the presence, degree and persistence of soil water repellency (SWR). Prolonged drought periods and wildfires can increase SWR substantially, thus the aim of this study was to determine the effect of forest fire-induced water repellency on soil hydraulic properties, infiltration and water flow in unsaturated soil (vadose) zone. Infiltration experiments with water and ethanol were conducted on forest sites, selected according to their exposure to fire: heavily burned (A), burned (B) and non-affected as the control site (C). Infiltration data were used as an input for inverse determination of soil hydraulic parameters required for computer model calibration (HYDRUS 2D/3D). Then, a one-year climatic scenario for 2016 with measured meteorological data was simulated using HYDRUS-1D software. Data showed that in the case of soil exposure to high temperatures (forest fires), a relatively large increase of SWR is observed. Compared to the control plot, a considerably greater difference between the hydraulic conductivity, K_s , values for water and ethanol was found at both fire affected plots. This suggested positive relationship between soil water repellency and reduced water infiltration. Numerical simulation of the intensive (extreme) rainfall event clearly showed that SWR affects soil water balance by reducing the infiltration and increasing the surface runoff.

Key words

soil hydrophobicity, soil infiltration, inverse modeling, soil water dynamics, HYDRUS

¹ University of Zagreb Faculty of Agriculture, Department of Soil Amelioration, Svetošimunska 25, 10000 Zagreb, Croatia

² University of Natural Resources and Life Sciences Vienna (BOKU), Institute of Hydraulics and Rural Water Management, Muthgasse 18, 1190 Vienna, Austria

✉ Corresponding author: lfilipovic@agr.hr

Received: February 6, 2019 | Accepted: April 17, 2019

Introduction

Climate change predictions are suggesting that redistribution of annual precipitation and prolonged dry periods with increased fire risk may be expected in the Mediterranean coastal area. Drought periods or wildfires can increase soil water repellency (SWR) substantially, thus its relevance for soil water dynamics will become more important (Weninger et al., 2019). SWR is defined as the contact or wetting angle (γ) between the soil particles and infiltrating water. Presence of SWR potentially reduces the infiltration and water retention in the soil (e.g., Filipović et al., 2018). Namely, if a drop of water is placed to the soil surface and it does not spontaneously infiltrate into the soil, the contact angle with the soil surface is greater than 90° , and therefore such soil is classified as hydrophobic. On the other hand, for hydrophilic soils is considered that they have the contact angle of 0 . However, the majority of soils are neither completely hydrophilic (wetable) or hydrophobic (repellent) but show a certain degree of SWR ($0 < \gamma < 90^\circ$) (Doerr et al., 2000; Letey et al., 2000). Although the level of SWR was linked to the quantity and possibly quality of soil organic particles (Goebel et al., 2011), due to the poor understanding of the exact chemical composition of the particles causing hydrophobicity and their mechanism of soil partitioning, the exact causes and characteristics of SWR still remain unclear. SWR is exceptionally variable and it is not a constant state of soil (Doerr et al., 2000), e.g., it increases with decreasing soil water content (Jordán et al., 2013; Schwen et al., 2015). SWR cannot be measured directly in the field, but has to be obtained indirectly, e.g., by observing the difference in flow behavior between water and a fully-wetting liquid, such as ethanol due to its specific physico-chemical properties (i.e. lower surface tension); which is why ethanol is commonly used for the estimation of SWR (i.e. zero repellency; Schwen et al., 2015).

Determination of soil hydraulic properties (SHP) in water repellent soils is an important issue, and research is especially

focusing on obtaining better modeling descriptions for simulations of various scenarios (Jarvis et al., 2008; Diamantopoulos and Durner, 2013; Chau et al., 2014; Schwen et al., 2015; Müller et al., 2018). Numerical models have become a standard tool for analyzing water flow in soil vadose zone (and transport of solutes, e.g., pollutants). Also, numerical modeling proved to be suitable tool for analyzing and predicting certain climatic and environmental scenarios (Šimůnek et al., 2016; Filipović et al., 2018). HYDRUS-1D and HYDRUS 2D/3D are computer software that allow simulation of one-, two- or three-dimensional movement of water, heat and various substances in a variable saturated media (soil), thus they are widely used for environmental modeling (Šimůnek et al., 2016).

The aim of this study was to estimate the effect of fire-induced water repellency on soil hydraulic properties and consequently water flow behavior. Data from the infiltration experiments were used as an input for the inverse determination of soil hydraulic parameters required for the calibration of HYDRUS 2D/3D model. After obtaining SHP, a one-year climatic scenario using HYDRUS-1D software was performed.

Materials and methods

The infiltration experiment was carried out in September 2016, near Žaborić (Šibenik, Croatia; $43^\circ 39' 39.6''$ N, $15^\circ 56' 49.2''$ E), on a brown soil on limestone and dolomite (Husnjak, 2014) where forest fires occurred in July 2016. Climatic data were collected on a daily basis from the meteorological station located at the nearby experimental field Jadrtovac (500 m from the forest fire site, using Pinova Meteo): mean annual precipitation was 631 mm, mean annual air temperature was 15.8°C , mean annual soil temperature was 16.0°C , and mean annual relative air humidity was 68.2 %. Three plots were selected in regard to their exposure to fire: (i) heavily burned - A, (ii) burned - B, and (iii) non-affected as the control site - C (Fig. 1).

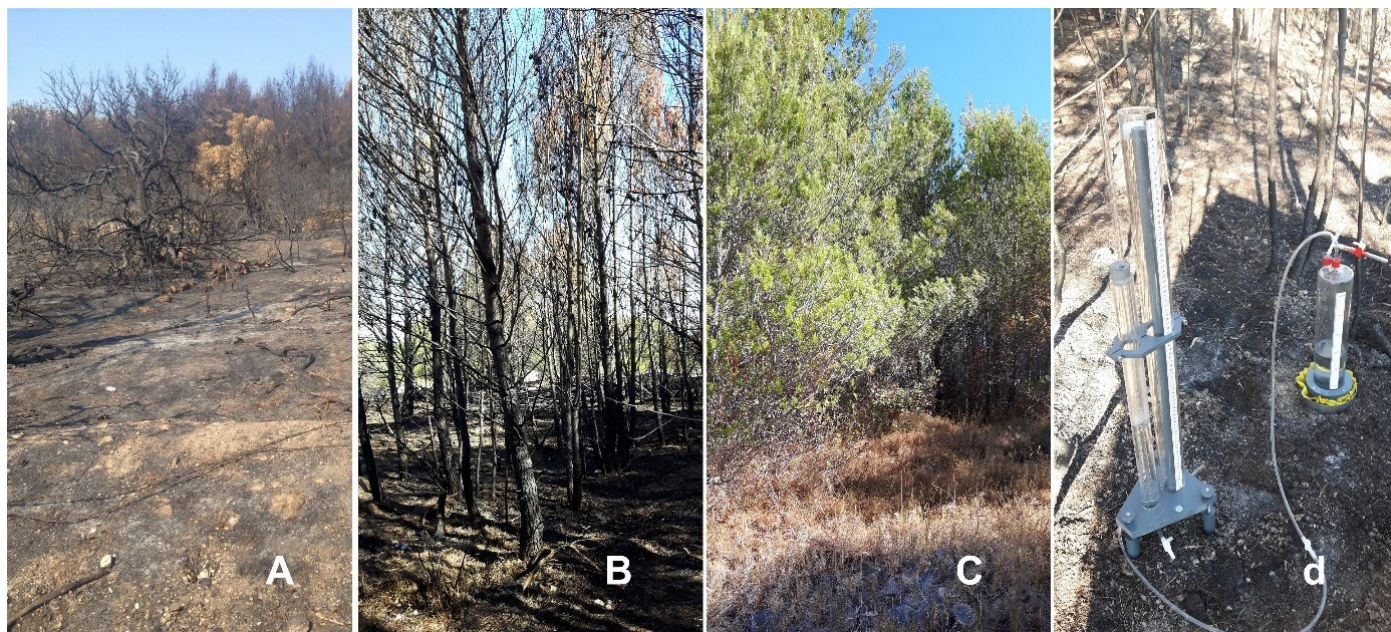


Figure 1. Experimental site near Šibenik, Croatia: (A) heavily burned plot, (B) burned plot, (C) control plot (non-affected by fire); and (d) the example of performed infiltration measurements.

Soil hydraulic properties at selected locations were estimated by measuring infiltration with water and ethanol as a fully-wetting liquid (three measurements per plot). Ethanol was used in SWR estimation due to its lower surface tension (i.e. zero repellency; Lamparter et al., 2010). Infiltration measurements were performed using a self-constructed tension disc glass infiltrometer with a 3000 ml reservoir (Schwen et al., 2015) at pressure heads of -10, -7, -3, and -1 cm (White et al., 1992). Organic residues were removed from the soil surface and glass beads were used (Dragonite Jaygo Inc., $\phi = 0.45$ mm) to provide a good hydraulic contact between the soil and the infiltrometer porous disc. Data for the total amount of fluid (water and ethanol) infiltrated in the topsoil were recorded over time and used for the inverse numerical determination of SHP (as described below). Additionally, subsoil hydraulic parameters were estimated according to the soil physical properties measured during previous survey at the experimental site Jadrtovac (distance 500 m). However, the subsoil was not in research focus because the main goal was to investigate the fire effect on soil infiltration and water repellency, both related to the properties of the first few centimeters of the topsoil (e.g., Badia-Villas et al., 2014).

Water and ethanol were used due to their differences in viscosity (η) ($\eta_{\text{water}} = 1.0$ mPa; $\eta_{\text{ethanol}} = 1.2$ mPa) and specific density (values presented below), which results in different infiltration rates. To be able to compare the two infiltration experiments, the infiltration rates of ethanol were corrected for the difference in viscosity between water and ethanol using a factor of 1.2 (Jarvis et al., 2008). Considering different physicochemical properties of water and ethanol, the ethanol pressure head values were scaled based on the capillary rise equation (Eq. 1, e.g., Jarvis et al., 2008) that takes into account the difference between surface tension and density of particular liquids:

$$h_i = \frac{2\sigma_i \cos \gamma}{r \rho_i g} \quad (1)$$

where σ is the surface tension (mN m^{-1}), γ is the contact angle ($^\circ$), r is the equivalent capillary radius (m), ρ is the density of the liquid (g cm^{-3}), and g is the acceleration due to gravity (m s^{-2}); the subscript i refers to water (w) or ethanol (e). With the water and ethanol surface tension at 20°C of 72.7 mN m^{-1} and 22.4 mN m^{-1} , and a density of 0.998 g cm^{-3} and 0.789 g cm^{-3} , respectively, a correction factor between h_e and h_w of 2.5 was assumed (Diamantopoulos et al., 2013; Lamparter et al., 2010). Multiplying h_e with 2.5 results in the effective supply pressure ($h_{e, \text{eff}}$) giving the applied ethanol pressure heads of -25, -12.5, -7.5, and -2.5 cm.

Soil water content measurement during the infiltration experiment was performed using a TDR 300 probe (FieldScout, Spectrum Technologies, Inc.). Using the probe (measurement at 0 - 15 cm depth) at the beginning and at the end of the implementation of each measurement, the relative amount of water in the soil and its change was determined with respect to the amount of liquid added by infiltration measurements.

Mathematical modeling was performed in two steps using HYDRUS 2D/3D and 1D model (Šimůnek et al., 2016): 1) inverse modeling based on water and ethanol field infiltration data was performed to determine the hydraulic characteristics of the soil (HYDRUS 2D/3D); 2) a direct modeling of seasonal simulation

(2016) was performed, to define the impact of SWR on soil water dynamics (HYDRUS 1D). The numerical solution of Richards equation, combined with the Levenberg-Marquardt nonlinear minimization method, was performed using HYDRUS (2D/3D) model. The program solves the equation numerically using a so-called pseudo-three-dimensional plane which uses one cross-section and takes into account that the assumption is correct for all 360° spatial domains. Richards equation was used in an altered form (Šimůnek et al., 1998):

$$\frac{\partial \theta}{\partial t} = \frac{1}{r} \frac{\partial}{\partial r} \left(r K \frac{\partial h}{\partial r} \right) + \frac{\partial}{\partial z} \left(K \frac{\partial h}{\partial z} \right) + \frac{\partial K}{\partial z} \quad (2)$$

where θ is the volumetric water content [$\text{L}^3 \text{L}^{-3}$], h is the pressure head [L], K is the unsaturated hydraulic conductivity [LT^{-1}], r is a radial coordinate [L], z is vertical coordinate [L], positive upwards, and t is time [T]. Equation (2) was solved numerically for the following initial and boundary conditions that reflect the initial and boundary conditions of the tension disc infiltrometer experiment:

$$\theta(r, z, t) = \theta_i \quad t = 0 \quad (3)$$

$$h(r, z, t) = h_0 \quad 0 < r < r_0, z = 0 \quad (4)$$

$$\frac{\partial h(r, z, t)}{\partial z} = -1 \quad r > r_0, z = 0 \quad (5)$$

$$h(r, z, t) = h_i \quad r^2 + z^2 \rightarrow \infty \quad (6)$$

where θ_i is the initial soil water content [$\text{L}^3 \text{L}^{-3}$], h_0 is the time variable supply pressure head imposed by the tension disc infiltrometer for water (-1, -0.5, -0.3, -0.1 kPa) and ethanol (-2.5, -1.25, -0.75, -0.25 kPa), [L], and r_0 is the disc radius (porous disc radius of 2.9 cm) [L]. The SHP, estimated from ethanol infiltration volumes (scaled to match water physicochemical properties), were assumed to reflect the water infiltration in hydrophilic soil. Soil hydraulic functions $\theta(h)$ and $K(h)$ used in the inverse and direct simulations (next section), were described using the van Genuchten-Mualem model (VGM; van Genuchten, 1980). Pore connectivity parameter (l) was fixed to 0.5 as recommended by Mualem et al. (1976) to avoid optimization of a large number of parameters.

The simulated domain was 15 cm in width and 20 cm in length of the soil block, with 2501 nodes and increased density at the upper boundary due to the position of the tension disk. The hydraulic parameters (residual water content, θ_r , saturated hydraulic conductivity, K_s , and empirical retention curve shape parameters α and n) were initially determined using the ROSETTA module that is embedded in the HYDRUS program (Schaap et al., 2001) (Table 1). Using the above-mentioned embedded function, the θ_r parameter has not been changed because the impact of this parameter on simulated θ and h time series is negligible (Šimůnek et al., 1998).

After the SHP determination based on the infiltration experiments and model validation by comparison with the field

Table 1. Initial van Genuchten-Mualem soil hydraulic parameters derived from pedotransfer functions (Rosetta, HYDRUS 1D) based on the particle size distribution.

Soil depth	θ_r	θ_s	α	n	K_s	l
cm	cm ³ cm ⁻³	cm ³ cm ⁻³	cm ⁻¹	-	cm ³ day ⁻¹	-
0 - 12	0.0485	0.3904	0.0075	1.5305	11.63	0.5
12 - 50	0.0916	0.4795	0.0088	1.493	11.84	0.5

θ_r – residual water content; θ_s – saturated water content; α and n – shape parameters; K_s – saturated hydraulic conductivity; l – pore connectivity parameter

measurements, a one-year simulation based on Richards equation in the HYDRUS-1D program was carried out (Šimůnek et al., 2016). For a one year simulation, the meteorological data from the nearby meteorological station (Jadrtovac) (i.e., evapotranspiration and rainfall) were used as a model input. Results of numerical simulations are compared with field values of infiltration volumes at different pressures using the coefficient of determination (R^2):

$$R^2 = \left(\frac{\sum_{i=1}^n (O_i - \bar{O})(S_i - \bar{S})}{\sqrt{\sum_{i=1}^n (O_i - \bar{O})^2} \sqrt{\sum_{i=1}^n (S_i - \bar{S})^2}} \right)^2 \quad (7)$$

where O_i and S_i are observed and simulated values, respectively, \bar{O} and \bar{S} are average observed and simulated values, respectively, and n is the number of observed/simulated points.

Additionally, soil water retention and hydraulic conductivity curves were determined from undisturbed soil samples (two per plot), taken at heavily burned (A), burned (B) and control (C) plot, using the HYPROP® system (METER Group AG) and a HYPROP-FIT software (HYPROP User Manual, 2018) based on the evaporation method (Schindler et al., 2010).

Results and discussion

Comparison of measured and simulated cumulative ethanol and water infiltration data is presented in Fig. 2. At investigated C plot, a rather typical water infiltration curve for non-repellent soils was observed (e.g., Šimůnek and van Genuchten, 1997), showing increased infiltration volumes at lower pressure heads (close to saturation). On the contrary, water infiltration at the A and B plots showed reduced infiltration at lower pressure heads ($h = -3$ cm and -1 cm) compared to the C plot, and had a steady slow inflow rate during the entire infiltration experiment, meaning that it did not respond to the change in applied pressure. At applied higher negative pressure, soil water flows through the smaller pores and the infiltration rate usually increases as the applied negative pressure is lowered because the larger pores also become active (e.g., control plot). Thus, no change in soil water inflow rate when lower negative pressure was applied indicated that the larger pores at the A and B plots were more hydrophobic than the smaller ones (Schwen et al., 2015). The total volume of infiltrated water in the soil was 205, 280 and 1130 ml at A, B and C plot, respectively. Furthermore, the infiltration volumes of ethanol were 2496, 2412 and 2448 ml at A, B and C plot, respectively. Such large difference between the infiltration rates of water and ethanol at A and B plots (ethanol infiltration was at A plot 12.2, and at B plot 8.6 times higher than the water infiltration) showed the presence of soil hydrophobicity, thus suggested that wildfire increased the

SWR substantially. Furthermore, although to a lesser extent than observed at the A and B plots, from the comparison of water and ethanol infiltration rates can be seen that the infiltration at C plot was also reduced (ethanol infiltration was 2.2 times higher than the infiltration of water). Thus, data also confirm that even in the absence of extreme events such as fire, some soils exhibit a certain level of water repellency (Doerr et al, 2000; Letey et al., 2000).

Soil water retention and saturated hydraulic conductivity curves based on HYPROP-FIT at A, B and C plots are shown in Fig. 3, with the black lines representing the prediction of the VGM curves. VGM curves had a similar shape for all three plots and thus suggested no difference between the plots. Here is important to note that the application of this method requires the initial complete saturation of the soil sample (Schindler et al., 2010), which reduces soil repellency (Diamantopoulos et al., 2013). Thus, these measurements were performed only to confirm that initially, before the forest fire event, there was no difference in soil water retention or hydraulic conductivity between the experimental plots (Fig. 3).

For this reason, data from the infiltration experiments (with different infiltrating liquids) were combined with the inverse numerical modeling in order to estimate the effect of SWR on water balance in the soil. Thus, based on the inversely optimized SHP at A, B and C plots shown in Table 2, new soil retention curves were reproduced for ethanol and water infiltration. Fig. 4 shows optimized soil retention curves obtained with the parameters shown and described in Table 2 for water (solid lines) and ethanol (dotted lines) infiltration measurements. Fitting of measured versus simulated data indicated that the model performance was reliable, with $R^2 > 0.94$ for all three plots. When the retention curves for water (${}_w$) are compared, the difference between fire affected (A and B) and control (C) plot was observed, with the greatest difference detected when sample passed from wet to dry phase, which is also when the highest values of SWR are usually expected (Filipović et al., 2018). Here, the difference in infiltration volumes between the plots and infiltrating liquids (water vs. ethanol) reflects the difference in soil hydraulic properties, which will cause a very different behavior of soil water flow. For example, when comparing water with ethanol infiltration, K_s was reduced by as much as 97.7 % at A and 98.8 % at B plot; and in contrast, by only 22 % at C plot (Table 2). Furthermore, data indicate that a certain degree of water repellency was also present at C plot, probably resulting from the uneven distribution of natural precipitation, e.g., during periods with a critically low water content (Jordán et al., 2013; Schwen et al., 2015), thus confirming the fact that the majority of the soils have a certain degree of SWR (Doerr et al., 2000).

After inverse modeling and determination of soil hydraulic

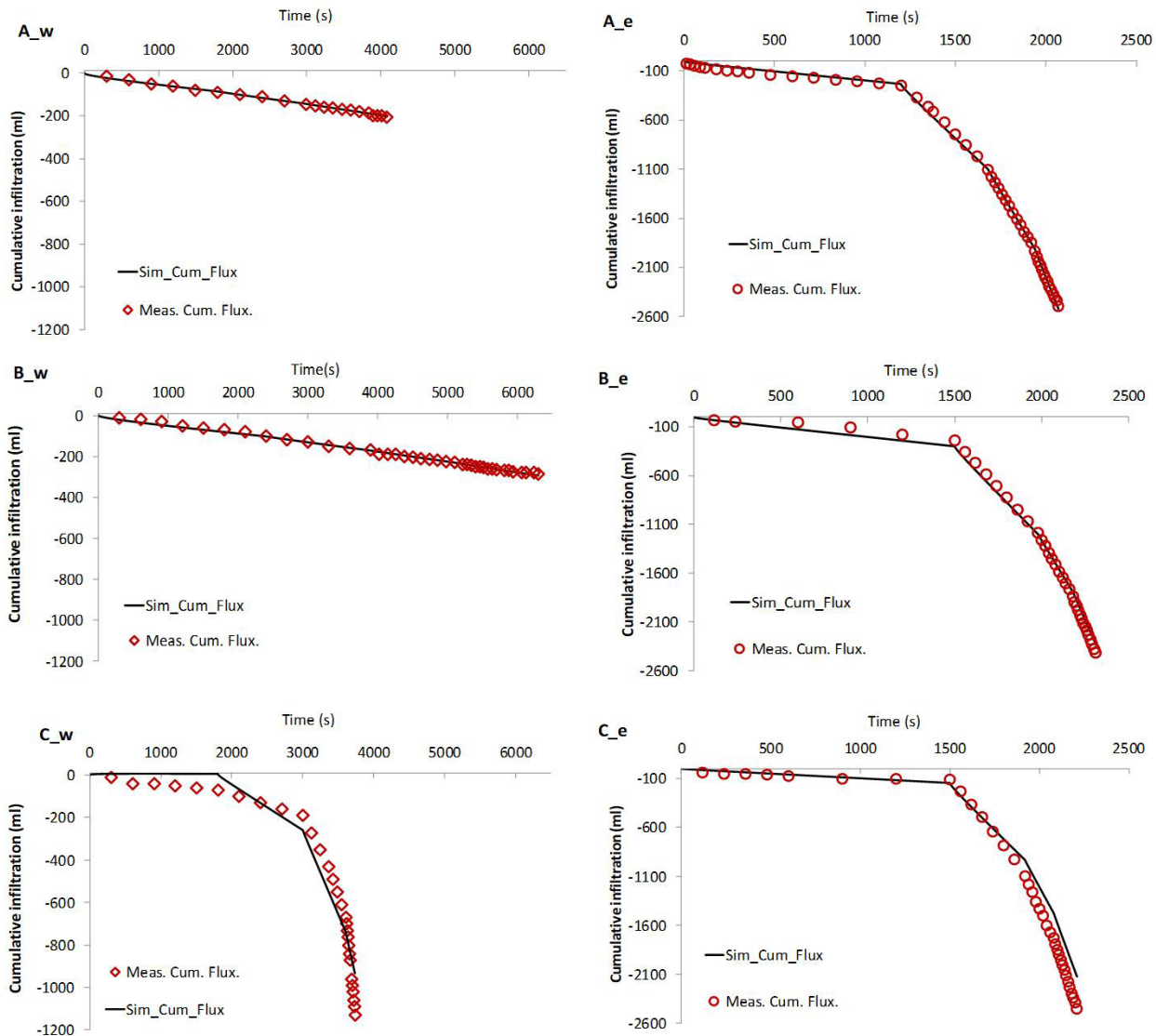


Figure 2. Measured (red rhombus and circles) and simulated (full line) values of cumulative ethanol (_e) and water (_w) infiltration at A (heavily burned), B (burned) and C (control) plots. Simulations were performed using inverse optimization procedure for water and ethanol in HYDRUS 2D/3D. Ethanol (_e) infiltration curves are optimized by taking into the account different physico-chemical properties and are directly comparable with water infiltration curves (_w).

parameters, direct simulation was performed using HYDRUS 1D program (one-year simulation with a daily temporal resolution, Fig. 5). In the simulations, initial SHP values shown in Table 1 were used for the subsoil, while parameters obtained with inverse modeling (Table 2) were used for the topsoil, for all three plots. Fig. 5 shows that simulated water content (at soil depth of 10 cm) is positively related to precipitation, reflecting increased water content in the topsoil at higher precipitation. The variations among the simulated water contents at the A, B and C plots are directly linked to the estimated hydraulic properties (α , n i K_s), but because of relatively low precipitation in 2016, the effect of high precipitation on soil water flow could not be tested. Thus, to test the effect of high precipitation event at A, B and C plots but still not deviate considerably from the real field situation, rainfall data for three days in September 2014 were added to the simulation of 2016. Time period from September 11 - 13, 2014 when an extreme precipitation event occurred (with total of 150 mm of rainfall)

Table 2. Van Genuchten-Mualem soil hydraulic parameters determined with the inverse procedure using HYDRUS (2D/3D) from field infiltrometer data measurements with water (_w) and ethanol (_e), with the indication of goodness of fit (R^2).

Plot_liquid	α cm ⁻¹	n -	K_s cm ³ day ⁻¹	R^2
A_w	0.017	1.334	33.93	0.996
A_e	0.042	3.625	1484.01	0.999
B_w	0.019	1.969	12.44	0.996
B_e	0.040	4.500	1072.66	0.998
C_w	0.172	4.500	1167.00	0.947
C_e	0.046	4.500	1495.67	0.998

α and n – shape parameters; K_s – saturated hydraulic conductivity

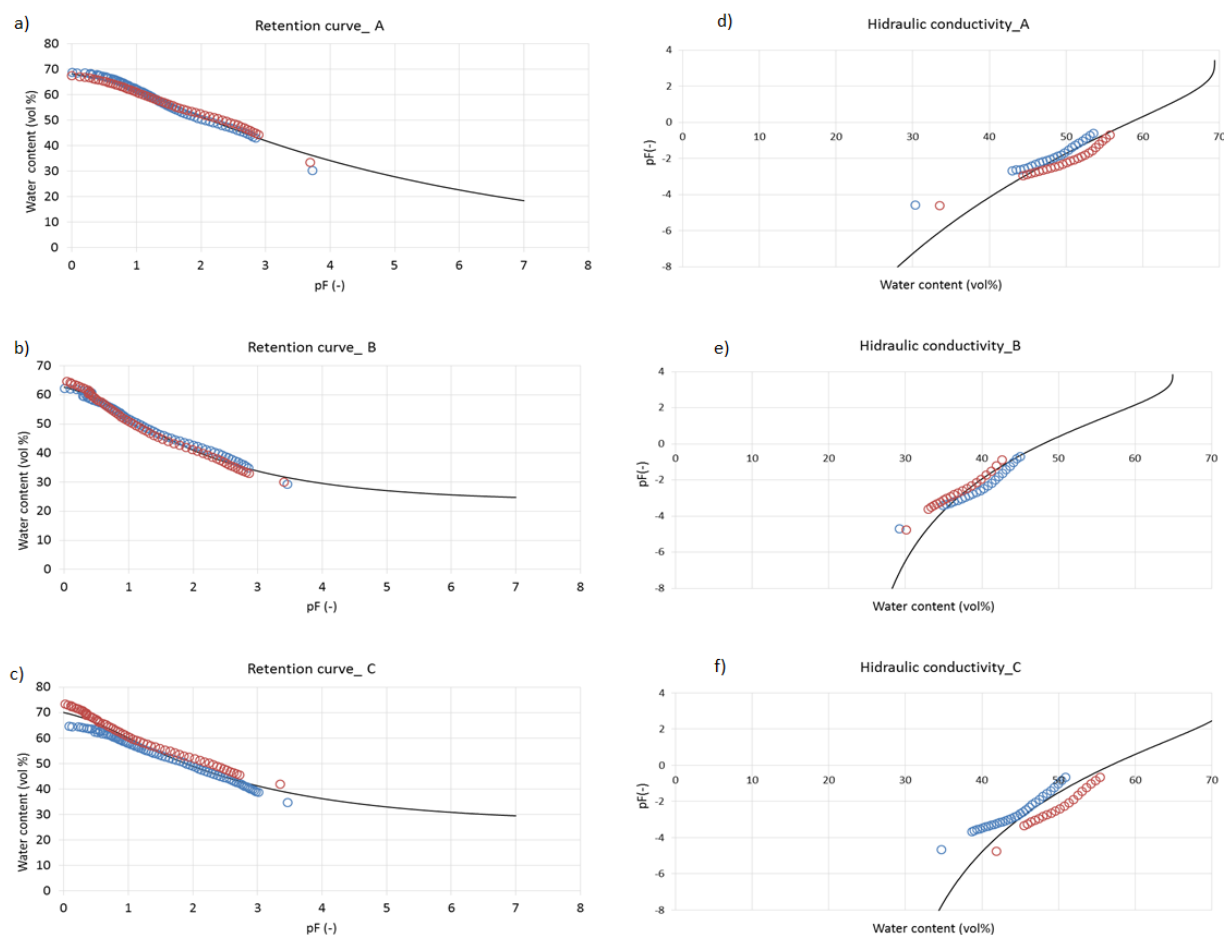


Figure 3. Soil water retention (a, b, c) and hydraulic conductivity curves (d, e, f) determined from undisturbed topsoil samples (5 - 10 cm) taken at heavily burned (A), burned (B) and control (C) plots using HYPROP-FIT computer program based on evaporation method. Black lines represent fitting curves based on the van Genuchten-Mualem model; red and blue circles represent measured data.

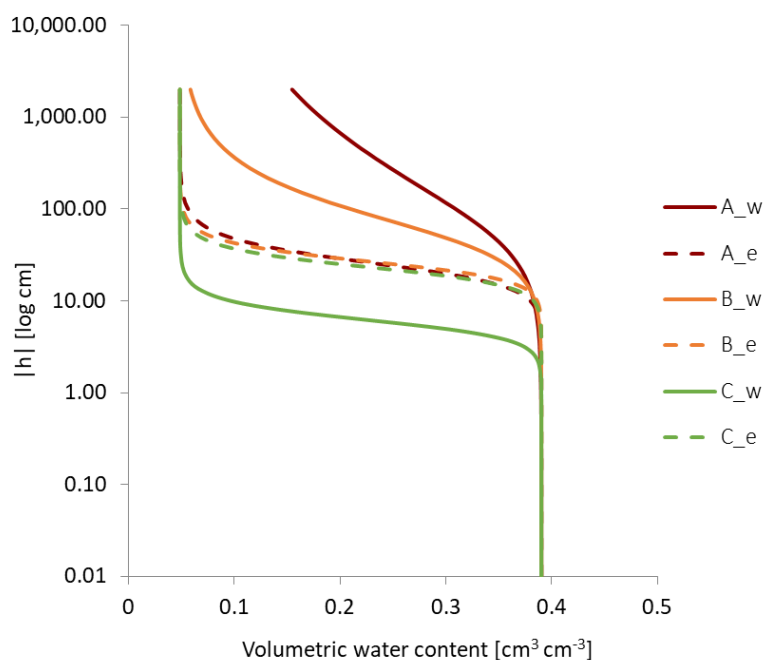


Figure 4. Soil retention curves for different van Genuchten-Mualem model hydraulic parameter sets for heavily burned (A), burned (B) and control (C) plots and different liquids (w, water vs. e, ethanol). Ethanol curves (_e) are scaled in order to take into account the different physicochemical properties and are directly comparable to water curves (_w).

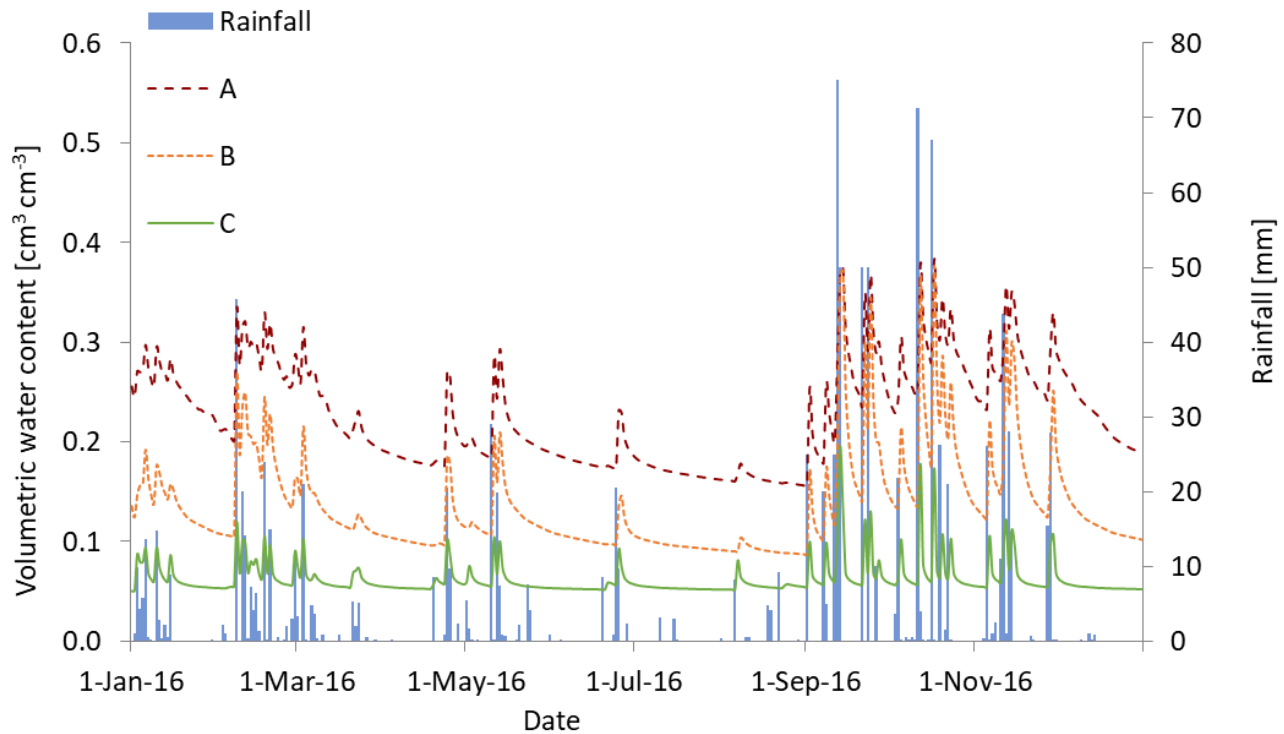


Figure 5. Simulated soil volumetric water content (at 10 cm) using HYDRUS 1D at A (heavily burned), B (burned) and C (control) plots; shown with the precipitation record (data from 2016 with increased precipitation for September 11 - 13, in accordance with the 2014 data).

was added to the simulation as if it reoccurred in September 11 - 13, 2016. Then, differences in the water balance between the fire affected (A and B) and control (C) plot were observed (Fig. 6). At the control (C) plot, no surface runoff was recorded because all simulated rainfall infiltrated the soil (15 cm).

On the other hand, reduced water infiltration in both fire affected

(hydrophobic) plots (A and B) was found, with the surface runoff higher than the amount of infiltrated water. Thus, data showed that, in the event of extreme precipitation, the infiltration of water into the soil is reduced because of SWR, while at the same time, as also shown in similar studies (e.g., Lemmnitz et al., 2008), surface runoff increases.

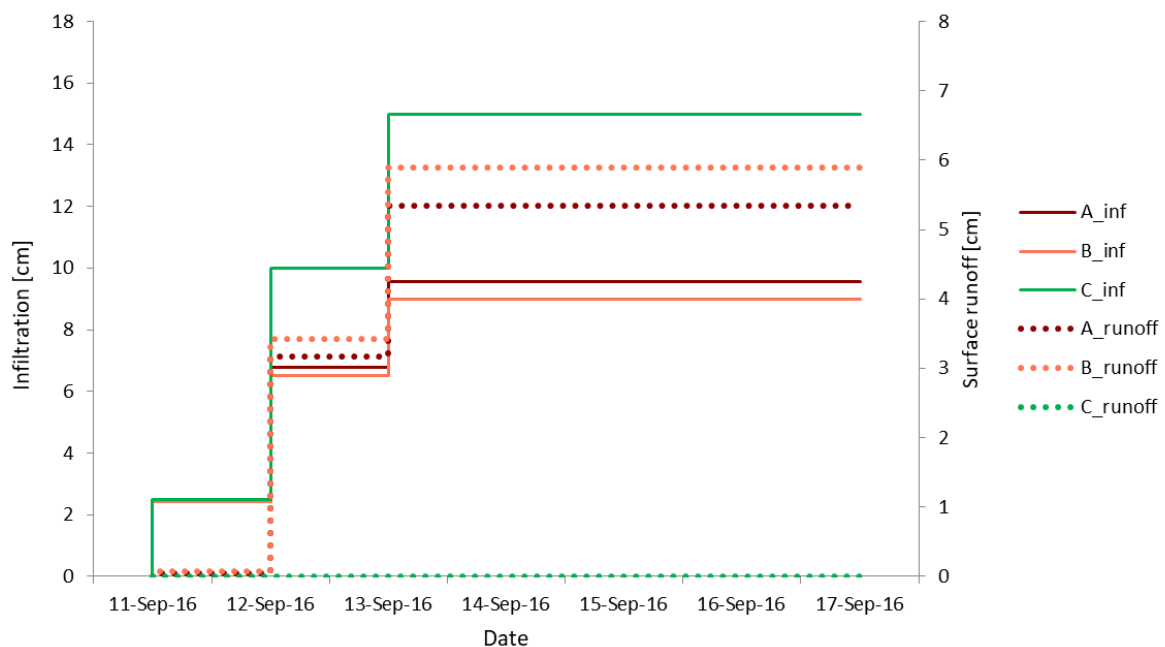


Figure 6. HYDRUS 1D simulation of soil water repellency effect on infiltration (full lines) and surface runoff (dotted lines) at A (heavily burned), B (burned) and C (control) plots after three days of intensive precipitation (September 11 - 13, in accordance with the 2014 data; with the cumulative precipitation of 150 mm).

Conclusion

Infiltration experiments with water and ethanol confirmed the presence of SWR at all three studied plots - heavily burned, burned and even at the control plot (non-affected by fire) to a certain extent, but with the SWR at the fire affected plots considerably more pronounced than at the control plot. Thus, data show that a relatively large increase of SWR is observed in the case of soil exposure to high temperatures (i.e., forest fires).

Compared to the control plot, a considerably greater difference between simulated K_s for water and ethanol (obtained with inverse modeling using HYDRUS 2D/3D; $R^2 > 0.94$) was found at both fire affected plots (heavily burned and burned). This suggested positive relationship between SWR and reduced water infiltration. Although it was not initially noticeable from the simulation for 2016, the additional simulation of three days with intensive precipitation (according to the extreme precipitation event recorded in 2014) clearly showed that SWR affects soil water balance by reducing the infiltration and enhancing surface runoff.

The overall results from this study suggest that, in the context of climate change and predicted increase in frequency and intensity of dry periods (usually associated with higher wildfire risk), it may be expected that the effect of SWR on hydrological processes will increasingly gain in relevance, especially in the Mediterranean region. Thus, further research focused on better understanding of the occurrence, degree and uneven nature of SWR is required.

References

- Badia-Villas, D., Gonzalez-Perez, J.A., Aznar, J.M., Arjona-Gracia, B., Marti-Dalmau, C., (2014). Changes in water repellency, aggregation and organic matter of a mollic horizon burned in laboratory: soil depth affected by fire. *Geoderma* 213, 400–407.
- Chau H. W., Biswas A., Vujanovic V., Si B.C. (2014). Relationship between the severity, persistence of soil water repellency and the critical soil water content in water repellent soils. *Geoderma* 221-222: 113-120
- Diamantopoulos E., Durner W. (2013). Physically-based model of soil hydraulic properties accounting for variable contact angle and its effect on hysteresis. *Adv. Water Resour* 59:169-180
- Diamantopoulos E., Durner W., Reszkowska A., Bachmann J. (2013). Effect of soil water repellency on soil hydraulic properties estimated under dynamic conditions. *J Hydrol* 486: 175-186
- Doerr S. H., Shakesby R. A., Walsh R. P. D. (2000). Soil water repellency: its causes, characteristics and hydro-geomorphological significance. *Earth-Sci Rev* 51: 33-65
- Filipović V., Weninger T., Filipović L., Schwen A., Bristow K. L., Zechmeister-Boltenstern S., Leitner S. (2018). Inverse estimation of soil hydraulic properties and water repellency following artificially induced drought stress. *J Hydrol Hydromech* 66 (2): 170-180
- Goebel M. - O., Bachmann J., Reichstein M., Janssens I. A., Guggenberger G. (2011). Soil water repellency and its implications for organic matter decomposition - is there a link to extreme climatic events? *Glob Change Biol* 17: 2640-2656
- Husnjak S. (2014). Sistematika tala Hrvatske. Hrvatska sveučilišna naklada. (in Croatian)
- HYPROP User Manual (2018). HYPROP User Manual v 2018/3. METER Group AG, 1-103
- Jarvis N., Etana A., Stagnitti F. (2008). Water repellency, near-saturated infiltration and preferential solute transport in a macroporous clay soil. *Geoderma* 143: 223-230
- Jordán A., Zavala L. M., Mataix-Solera J., Doerr S. H. (2013). Soil water repellency: origin, assessment and geomorphological consequences. *Catena* 108: 1-5
- Lamparter A., Bachmann J., Deurer M., Woche S. K. (2010). Applicability of ethanol for measuring intrinsic hydraulic properties of sand with various water repellency levels. *Vadose Zone J* 9: 445-450
- Lemmnitz C., Kuhnert M., Bens O., Guntner A., Merz B., Huttl R. F. (2008). Spatial and temporal variations of actual soil water repellency and their influence on surface runoff. *Hydrol process* 22: 1976-1984
- Letey J., Carrillo M. L. K., Pang X. P. (2000). Approaches to characterize the degree of water repellency. *J Hydrol* 231-232: 61–65
- Mualem Y. (1976). A new model for predicting the hydraulic conductivity of unsaturated porous media. *Water Resour Res* 12 (3): 513-521
- Müller K., Mason K., Strozzi A. G., Simpson R., Komatsu T., Kawamoto K., Clothier B. (2018). Runoff and nutrient loss from a water-repellent soil. *Geoderma* 322: 28-37
- Schaap M. G., Leij F. J., van Genuchten M. T. (2001). ROSETTA: a computer program for estimating soil hydraulic parameters with hierarchical pedotransfer functions. *J Hydrol* 251: 163-176
- Schindler U., Durner W., von Unold G., Müller L. (2010). Evaporation Method for Measuring Unsaturated Hydraulic Properties of Soils - Extending the Measurement Range. *Soil Sci Soc Am J* 74 (4): 1071-1083
- Schwen A., Zimmermann M., Leitner S., Woche S. K. (2015). Soil Water Repellency and its Impact on Hydraulic Characteristics in a Beech Forest under Simulated Climate Change. *Vadose Zone J* 14-12: 1-11
- Šimůnek J., Angulo-Jaramillo R., Schaap M. G., Vandervaere J. P., van Genuchten M. T. (1998). Using an inverse method to estimate the hydraulic properties of crusted soils from tension disc infiltrometer data. *Geoderma* 86: 61-81
- Šimůnek J., van Genuchten, M. T., Šejna M. (2016). Recent Developments and Applications of the HYDRUS Computer Software Packages. *Vadose Zone J* 15 (7): 25 p. DOI: 10.2136/vzj2016.04.0033
- Šimůnek J., van Genuchten M. T. (1997). Parameter estimation of soil hydraulic properties from multiple tension disc infiltrometer data. *Soil Sci* 162: 383-398
- Van Genuchten M. T. (1980). A closed-form equation for predicting the hydraulic conductivity of unsaturated soils. *Soil Sci Am J* 44: 892-898
- Weninger T., Filipović V., Mešić M., Clothier B., Filipović L. (2019). Estimating the extent of fire induced soil water repellency in Mediterranean environment. *Geoderma* 338: 187-196
- White I., Sully M. J., Perroux K. M. (1992). Measurement of surface-soil hydraulic properties: disk permeameters, tension infiltrometers, and other techniques. *Advances in Measurement of Soil Physical Properties: Bringing Theory into Practice*. Soil Science Society of America Special Publication no. 30, Madison, WI, USA: 69-103